Angewandte
Chemie

Metal–Metal Bonding

DOI: 10.1002/anie.200705257

Electron-Density Investigation of Metal–Metal Bonding in the Dinuclear "Borylene" Complex [{Cp(CO)₂Mn}₂(μ-B*t*Bu)]**

Ulrike Flierler, Michael Burzler, Dirk Leusser, Julian Henn, Holger Ott, Holger Braunschweig, and Dietmar Stalke

Dedicated to Professor Peter Luger on the occasion of his 65th birthday

Numerous examples in the past decade showed the borylene B−R moieties to be valuable alternatives to the isolobal and ubiquitous carbonyl C=O ligand in organometallic chemistry.[1] Computational studies identified the borylene moieties to give thermodynamically more stable transition-metal complexes than the carbonyl ligand in terms of homolytic cleavage of the respective metal–element bond.[2] In addition, the coordination mode of borylene moieties in multinuclear complexes is very flexible and varies from terminal to μ and μ₃ bridging.

We chose [{Cp(CO)₂Mn}₂(μ-B*t*Bu)][3] (**1**, Cp = C₅H₅; Figure 1) as a model compound for the investigation of the metal–metal bonding in bridged and non-bridged organometallic complexes. When formulating the Lewis structure of **1**, it is tempting to draw a "bond" between the two manganese

Figure 1. Molecular structure of **1** (anisotropic displacement parameters are depicted at the 50% probability level; hydrogen atoms are omitted for clarity).

[*] U. Flierler, Dr. D. Leusser, Dr. J. Henn, H. Ott, Prof. Dr. D. Stalke
Institut für Anorganische Chemie der Universität Göttingen
Tammannstrasse 4, 37077 Göttingen (Germany)
Fax: (+49) 551-39-3459
E-mail: dstalke@chemie.uni-goettingen.de
Homepage: http://www.stalke.chemie.uni-goettingen.de

Dr. M. Burzler, Prof. Dr. H. Braunschweig
Institut für Anorganische Chemie der Universität Würzburg
Am Hubland, 97074 Würzburg (Germany)

atoms to satisfy the 18-electron-rule.[4] This assumption seems further justified by the short distance between the two manganese atoms (2.78 Å) and the acute Mn-B-Mn angle (87°). In addition, there is no evidence for unpaired electrons in the complex.[5] The bonding situation was described to be of the borylene type and therefore to resemble that of carbonyl-bridged transition-metal complexes. Consequently, a three-center–two-electron (3c2e) bond would be expected with an "electron lobe" from the boron atom being directed at the Mn–Mn midpoint.[3,6]

As the experimental X-ray determination of accurate electron densities (EDs) made great progress during the past decades,[7] it has become a widely applied technique for structural description and further analyses. This holds even for transition-metal complexes, which have a much lower suitability index[6] than other small molecules. Together with a topological analysis according to Bader's quantum theory of atoms in molecules (QTAIM)[8] the X-ray determination can serve as an incisive tool for the derivation of density-based properties such as bond paths (BPs) and bond critical points (BCPs), and therefore help when deciding on the presence or absence of a bond.

The electronic structure of **1** was investigated by a low-temperature high-resolution X-ray diffraction experiment and a subsequent multipole refinement. The topological analysis of the ED distribution obtained provides a totally different picture of the bonding situation than that derived from simple geometrical considerations.

Surprisingly, neither in the experiment nor from calculations at the bp/TZVP[9] level of theory was a BP (and correspondingly a BCP) found between the two manganese atoms. Therefore, the compound stands in close relationship to its carbonyl-bridged analogues. The absence of BPs in supported di- or multinuclear transition-metal complexes is well known and has been subject of several studies.[6] Recently, there has been some discussion, if the absence of a bond path implies the absence of a bond.[10] Only slight variations in the geometry of semibridged iron carbonyl complexes cause the abrupt disappearance of the BP while other bond descriptors change in a physically more meaningful way.[11] Apparently, the formation of a BP can also be averted by a general raising of the level of the density in the bonding region in three-membered rings.[12]

An examination of the total electron density ρ(**r**) (Figure 2a) already reveals an indentation in the Mn–Mn region and the orthogonal gradient-vector trajectories (Figure 2b) explain why the formation of an Mn–Mn BP is prevented:
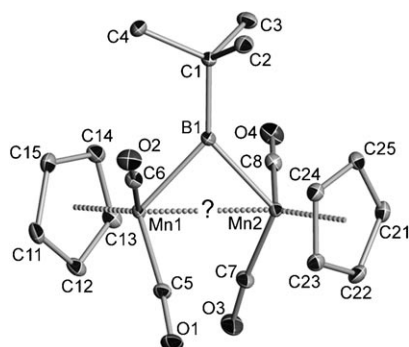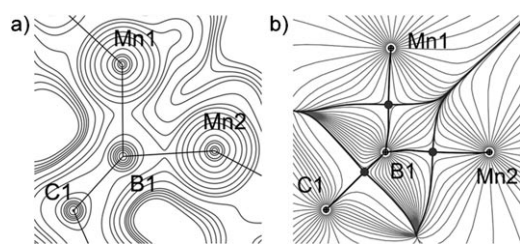
Figure 2. a) Total electron density $\rho(\mathbf{r})$ and b) trajectory field in the Mn$_2$B plane of **1** (BPs: black lines; gradient vector field lines: gray lines; BCPs: black dots).

The atomic basin of the boron atom spreads out between the two manganese basins and inhibits the formation of a saddle point in $\rho(\mathbf{r})$.

An inspection of the Laplacian distribution reveals differences compared to the carbonyl-bridged species. It shows three valence shell charge concentrations (VSCCs) at the boron atom (Figure 3a and g). These VSCCs are close to the vectors linking the bonded neighbors. In contrast, the Laplacian distribution of symmetrical, μ-bridged species, such as [Co$_2$(CO)$_8$] (**2**), shows only two VSCCs; one of these VSCCs points at the carbonyl oxygen atom, while the other one is broadened and directed towards the Co–Co midpoint (Figure 3b).

In the vicinity of each manganese atom in **1** six charge concentrations (CCs) are detected in a distorted octahedral geometry, one of the CCs faces a VSCC at the boron atom (Figure 3a), indicating contributions of shared interactions.

Ligand-induced charge concentrations (LICCs) are found *trans* as well as *cis* to the bonding CC.[13] The VSCCs of the carbon atoms of the carbonyl groups face charge depletions at the manganese atoms (Figure 3c). The Cp coordination is made up of a CC at the corresponding manganese atom oriented towards the ring center, while the VSCCs at the ring carbon atoms are outside the straight Mn–C bond paths (Figure 3d). The outer-shell structure of the manganese atoms, showing well resolved charge concentrations and depletions (Figure 3e) is indicative of the superb quality of the data.

The arrangement and related values of the CCs coincide with the calculated d-orbital populations from the refined multipole parameters.[14] The orbital population analysis leads to net charges of −0.73 and −0.76e on the two manganese atoms. The d$_{z^2}$ orbital reveals the highest population reflecting the predominant contribution of this orbital to the Mn−Cp bonds (Table 1). Therefore the shape of this orbital is mimicked by the static deformation density distribution (Figure 3f).[15]

Focusing on the metal–metal interaction, the source function (SF)[16] provides a very efficient tool for the analysis

Table 1: d-Orbital populations in [e] from the multipole parameters.[14]

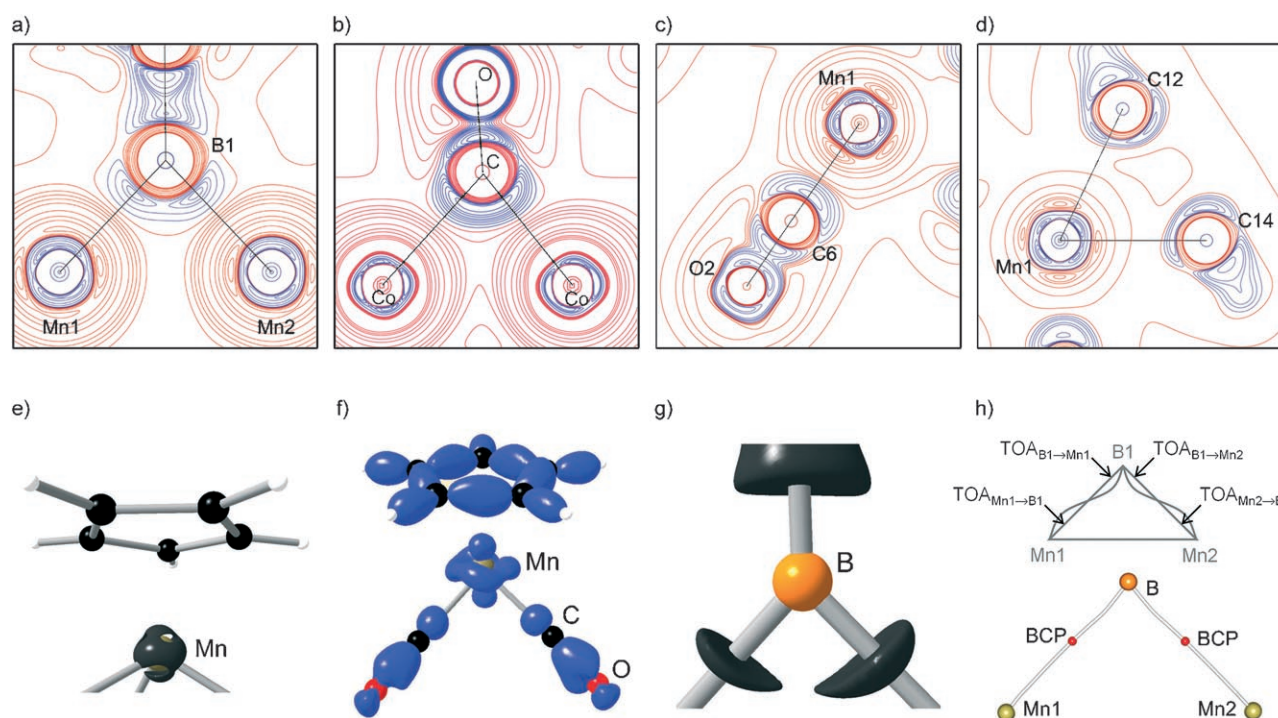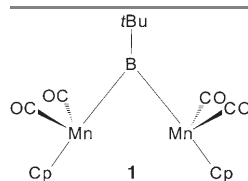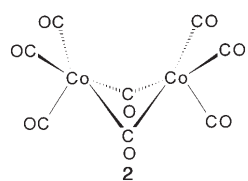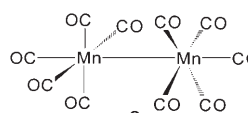|	z^2	xz	yz	x^2-y^2	xy
Mn1	1.51	0.91	0.79	1.33	1.19
Mn2	1.43	0.81	0.88	1.24	1.37

Figure 3. $\nabla^2\rho(\mathbf{r})$ in the Mn$_2$B plane (a), for comparison in the Co$_2$CO plane of **2** (b; reproduced with permission from ref. [6]), in the Mn1-C6-O2 plane (c), and in the Mn1-C12-C14 plane (d); blue lines indicate negative values in $\nabla^2\rho(\mathbf{r})$, red lines stand for positive values), isosurface representation of $\nabla^2\rho(\mathbf{r})$ (e), and static deformation density (f) around one manganese atom, isosurface representation of $\nabla^2\rho(\mathbf{r})$ at the boron atom (g), and the Mn$_2$B triangle defining the take off angles (TOA) (h, top) and depicting the BPs and BCPs (h, bottom). The graphics for the manganese complex are derived from experimental data.

of ED distributions. It is suitable for determining the contribution of functional groups to the electron density at defined points, for example, at BCPs, and allows the quantification of weak interactions, such as hydrogen bridges[17] or metal–metal bonds,[18] where the topological indicators are not as decisive as in classical 2c2e bonds.

Owing to the non-existent BCP, the local SF was determined on experimentally as well as theoretically derived charge distributions along the Mn–Mn vector (Figure 4) with the midpoint (MP)[18] taken as the reference point. The density at the MP was determined to be 0.2 e Å^{-3}. The property profiles derived from theory and experiment show a very good agreement. The Laplacian remains positive in a large interval around the midpoint and consequently the SF is negative in the same range.

Table 2: Experimental and *theoretical* topological features of **1** and the related key metal carbonyls **2**[18, 21] and **3**[20], at the M–M midpoint for **1** and **2** and at the BCP for **3**.

Complex	d(M–M) [Å]	$\rho(\mathbf{r})$ [eÅ^{-3}]	$\nabla^2\rho(\mathbf{r})$ [eÅ^{-5}]	G	$|V|$	$|V|/G$
1	2.782	0.217	1.428	0.019	0.014	0.737
	2.807	*0.263*	*0.952*	*0.020*	*0.024*	*1.200*
2	2.538	–[a]	–	–	–	–
	2.548	*0.311*	*2.101*	*0.035*	*0.048*	*1.371*
3	2.903	0.144	0.720	0.014	0.012	0.857
	2.906	*0.200*	*-0.071*	*0.009*	*0.017*	*1.889*

[a] For **2** no further experimental values are available because the charge density study in ref. [21] did not include a QTAIM analysis.
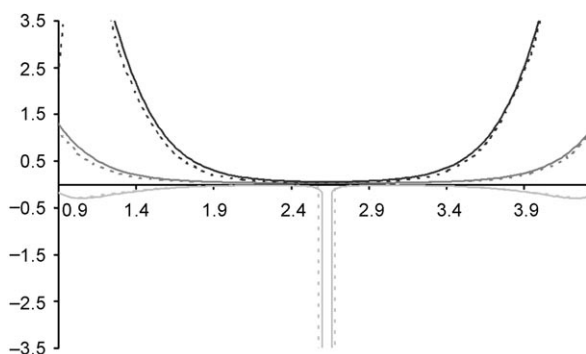

Figure 4. Property profiles along the metal–metal vector, horizontal axis: bond length (black: $\nabla^2\rho(\mathbf{r})$; dark gray: $\rho(\mathbf{r})$; light gray: local SF each in [a.u.]; dashed lines represent theoretical data).

In addition, the integrated SF was examined to determine the density contributions at the MP. More than 50% of the density at the MP is contributed by the carbonyl groups, whereas the bridging boron atom subtracts density from the MP (S(B) = −11.69%).

Following the arguments of Gatti and Lasi, the SF of **1** depicts the Mn−Mn bond as strongly nonlocalized,[19] because the metal atoms serve as sinks (S(Mn1) = −9.27% and S(Mn2) = −7.93%) rather than being sources of bonding density.[18] According to the bond descriptors shown in Table 2 the Mn–Mn distance in **1** is shorter and the density at the midpoint accordingly higher than in [Mn$_2$(CO)$_{10}$] (**3**), which is commonly believed to show a Mn−Mn bond. However, the ratio |V|/G, which classifies bonding by energy density considerations, is the smallest in the series [Mn$_2$(CO)$_{10}$][20] (**3**), [Co$_2$(CO)$_8$][18,21] (**2**), and [{Cp(CO)$_2$Mn}$_2$(μ-B*t*Bu)] (**1**).

Since the missing bond path contradicts the presence of a classical 2c2e Mn−Mn bond, the nature of the Mn−B interactions gain additional importance. The geometrical arrangement around the boron atom shows no striking features apart from the acute Mn-B-Mn angle. The B−C bond length (1.61 Å) lies in the range quoted for *tert*-butylboranes.[3] The two Mn−B bonds have identical lengths (2.02 Å). The density-related properties at the BCPs are uncontroversial, with density values of 0.61 and 0.65 e Å^{-3} and Laplacian values of 1.22 and 1.19 e Å^{-5}. The BCPs are shifted about 0.08 Å from the nonpolar midpoint[6] towards the boron atom, a situation which contradicts the differences in the electronegativities. This feature is a strong indication of density polarization towards the manganese atoms.

The build-up of positive charge at the boron atom, as predicted by DFT calculations,[3] is confirmed by the integrated charge (+1.04 e) from the QTAIM analysis of the experimental ED distribution. The positive charge implies a kinetical lability and a susceptibility for nucleophilic cleavage of the Mn−B bond, which is stabilized solely by the sterically demanding *t*Bu group.[2]

The integrated charges are close to zero for the manganese atoms, −0.43 e for the central carbon atom C1, and still −0.35 e for the whole *t*Bu group. In sum, they are overcompensated by the positive charge at the boron atom, because the B-*t*Bu moiety adds up to +0.69 e. Inspection of the group charges of the two Cp rings (−0.09 and +0.24 e) reveals a molecular asymmetry. The positive charges have to be counterbalanced primarily by the four carbonyl groups. Interestingly, the CO group charges differ from approximately zero (C5−O1 and C7−O3) to −0.24 and −0.27 e (C6−O2 and C8−O4, respectively). This asymmetry is mirrored in the signals for the Cp and CO ligands in the IR spectrum

(calcd $\tilde{v}$ [cm^{-1}] Cp$_{rot.}$ 28.0 and 54.7; CO$_{stretch.}$ 1900.6, 1916.0 (asym.) and 1937.1, 1968.9 (sym.)).

The Mn–B bond paths are curved (Figure 3h). Interestingly, the deviations from the straight paths, quantified by the take-off angle (TOA), are in the same range at the boron atom (TOA$_{B1\rightarrow Mn1}$ = 5.81°, TOA$_{B1\rightarrow Mn2}$ = 4.97°) but not symmetrical at the two manganese atoms (TOA$_{Mn1\rightarrow B1}$ = 7.37°, TOA$_{Mn2\rightarrow B1}$ = 12.11°). These angles reflect the relative contributions of direct B→Mn donation in comparison to the B←Mn back-donation.[6,15] The sum of the TOAs at the boron atom is 10.78° and thus only about half the value found at the manganese atoms (19.48°), indicating a dominant direct symmetrical B→Mn donation in contrast to less pronounced and nonsymmetrical B←Mn back-donation.

In the framework of Bader's QTAIM, the interpretation of the experimentally and theoretically derived electron density for **1** both exclude the existence of a Mn–Mn bond. However, this result cannot unambiguously be deduced from the indecisive bond descriptors employed. As in other examples, the density distribution in the triangular motif might prevent the formation of a bond path. With this complex however, the Mn–B bonding shows that electron pairing is accomplished through the boron atom and hence bonding is delocalized. The bond paths to the boron ligand serve as preferred exchange channels[22] and preclude the postulation of a diradical. Hence the findings are in tune with the experimental diamagnetic nature of the complex.

In summary, the apparently simple question of bonding between the metal atoms still cannot be answered ultimately by the present bond descriptors. Clearly, further experiments on the complex metal–metal bonding will provide even more sophisticated bond descriptors and point the way to more resilient concepts. The Laplacian distribution around the boron atom with its three VSCCs clearly shows the difference between the borylene ligand and the carbonyl ligand. Consequently, **1** clearly has to be classified as a dimetallaborane rather than a borylene complex.

Experimental Section

The diffraction data were collected at 100 K[23] on a Bruker TXS-Mo rotating anode with INCOATEC Helios mirror optics and APEX II detector. A high-resolution data set was obtained (($\sin\theta/\lambda$)$_{max}$ = 1.19 Å^{-1}; redundancy = 7.67 at 95.4% completeness up to ($\sin\theta/\lambda$)$_{max}$ = 1.19 Å^{-1}). The data collection was monitored with the APEX2 package,[24] the integration was performed with SAINT.[25] The data were corrected for absorption, scaled, and merged with the SADABS 2006/4 version,[26] which was modified for charge-density data purposes (183 988 total and 23 866 unique reflections; R_{int} = 0.0312).

The structure was solved with SHELXS[27] and a conventional refinement using all data was performed with SHELXL-97.[28] After an independent atom model (IAM) refinement, a multipole refinement on F^2 was performed using the atom-centered multipole model by Hansen and Coppens.[29] This procedure was carried out with the full-matrix-least-squares refinement program XDLSM implemented in the XD2006 package.[30] Several models, differing in the degree of chemical constraints applied and local noncrystallographic symmetry restrictions were refined and compared. The model which led to the lowest R-values ($R_{all}\{F^2\}$ = 0.0182; N_{ref}/N_{para} = 24.12) and a flat and featureless residual density at minimal correlations was selected for the discussion.

A full gas-phase optimization was carried out employing the bp exchange-correlation functional and the TZVP basis set with Turbomole.[31] The optimization yields an elongated Mn–Mn distance, reflecting a flat energy potential surface with respect to small changes in the Mn–Mn distance and the shortcomings of the density functional. For the topological analysis AIM2000[32] was used.

Further experimental details on data acquisition, processing, and refinement can be found in the Supporting Information section under http://www.angewandte.org or from the author.

[1] a) H. Braunschweig, *Angew. Chem.* **1998**, *110*, 1882; *Angew. Chem. Int. Ed.* **1998**, *37*, 1786; b) H. Braunschweig, M. Colling, *Coord. Chem. Rev.* **2001**, *223*, 1; c) H. Braunschweig, C. Kollann, D. Rais, *Angew. Chem.* **2006**, *118*, 5380; *Angew. Chem. Int. Ed.* **2006**, *45*, 5254; d) H. Braunschweig, *Adv. Organomet. Chem.* **2004**, *51*, 163; e) H. Braunschweig, M. Colling, *Eur. J. Inorg. Chem.* **2003**, 393; f) S. Aldridge, D. L. Coombs, *Coord. Chem. Rev.* **2004**, *248*, 535.

[2] a) A. W. Ehlers, E. J. Baerends, M. F. Bickelhaupt, U. Radius, *Chem. Eur. J.* **1998**, *4*, 210; b) C. Boehme, J. Uddin, G. Frenking, *Coord. Chem. Rev.* **2000**, *197*, 249; c) M. Blank, C. Colling, C. Kollann, K. Radacki, D. Rais, K. Uttinger, G. R. Whittell, *Chem. Eur. J.* **2007**, *13*, 4770.

[3] a) H. Braunschweig, T. Wagner, *Angew. Chem.* **1995**, *107*, 904; *Angew. Chem. Int. Ed. Engl.* **1995**, *34*, 825; b) H. Braunschweig, C. Burschka, M. Burzler, S. Metz, K. Radacki, *Angew. Chem.* **2006**, *118*, 4458; *Angew. Chem. Int. Ed.* **2006**, *45*, 4352.

[4] a) N. V. Sidgwick, *Electronic Theory of Valency*, Oxford University Press, Oxford, **1927**; b) C. Elschenbroich, A. Salzer, *Organometallics—A Concise Introduction*, VCH, Weinheim, **1992**.

[5] Neither EPR spectroscopy at liquid-N$_2$ temperature (77 K) nor SQUID measurements from room temperature to 4 K show any paramagnetic behavior arising from unpaired electrons in the bulk material.

[6] P. Macchi, A. Sironi, *Coord. Chem. Rev.* **2003**, *238–239*, 383.

[7] a) P. Coppens, *Angew. Chem.* **2005**, *117*, 6970; *Angew. Chem. Int. Ed.* **2005**, *44*, 6810; b) H. Ott, D. Stalke, *Nachr. Chem.* **2008**, *56*, 131.

[8] R. F. W. Bader, *Atoms in Molecules—A Quantum Theory*, Oxford University Press, New York, **1990**.

[9] a) A. Schäfer, C. Huber, R. Ahlrichs, *J. Chem. Phys.* **1994**, *100*, 5829; b) J. P. Perdew, *Phys. Rev. B* **1986**, *33*, 8822; c) A. D. Becke, *Phys. Rev. A* **1988**, *38*, 3098.

[10] L. J. Farrugia, C. Evans, M. Tegel, *J. Phys. Chem. A* **2006**, *110*, 7952.

[11] P. Macchi, L. Garlaschelli, A. Sironi, *J. Am. Chem. Soc.* **2002**, *124*, 14173.

[12] J. Henn, D. Leusser, D. Stalke, *J. Comput. Chem.* **2007**, *28*, 2317.

[13] W. Scherer, P. Sirsch, D. Shorokhov, M. Tafipolsky, G. S. McGrady, E. Gullo, *Chem. Eur. J.* **2003**, *9*, 6057.

[14] A. Holladay, P. Leung, P. Coppens, *Acta Crystallogr. Sect. A* **1983**, *39*, 377.

[15] W. Scherer, G. Eickerling, D. Shorokhov, E. Gullo, G. S. McGrady, P. Sirsch, *New J. Chem.* **2006**, *30*, 309.

[16] R. F. W. Bader, C. Gatti, *Chem. Phys. Lett.* **1998**, *287*, 233.

[17] a) C. Gatti, L. Bertini, *Acta Crystallogr. Sect. A* **2004**, *60*, 438; b) C. Gatti, F. Cargnoni, L. Bertini, *J. Comput. Chem.* **2003**, *24*, 422; c) J. Overgaard, B. Schiøtt, F. K. Larsen, B. B. Iversen, *Chem. Eur. J.* **2001**, *7*, 3756; d) J. Sørensen, H. F. Clausen, R. D. Poulsen, J. Overgaard, B. Schiøtt, *J. Phys. Chem. A* **2007**, *111*, 345.

[18] C. Gatti, D. Lasi, *Faraday Discuss.* **2007**, *135*, 55.

[19] J. D. Dunitz, A. Gavezzotti, *Angew. Chem.* **2005**, *117*, 1796; *Angew. Chem. Int. Ed.* **2005**, *44*, 1766.

[20] a) R. Bianchi, G. Gervasio, D. Marabello, *Chem. Commun.* **1998**, 1535; b) R. Bianchi, G. Gervasio, D. Marabello, *Inorg. Chem.* **2000**, *39*, 2360; c) L. J. Farrugia, P. R. Mallinson, B. Stewart, *Acta Crystallogr. Sect. B* **2003**, *59*, 234.

[21] a) P. C. Leung, P. Coppens, *Acta Crystallogr. Sect. B* **1983**, *39*, 535; b) G. Gardner Sumner, H. P. Klug, L. E. Alexander, *Acta Crystallogr.* **1963**, *17*, 732.

[22] a) A. M. Pendás, E. Francisco, M. A. Blanco, C. Gatti, *Chem. Eur. J.* **2007**, *13*, 9362; b) J. Reinhold, O. Kluge, C. Mealli, *Inorg. Chem.* **2007**, *46*, 7142.

[23] a) T. Kottke, D. Stalke, *J. Appl. Crystallogr.* **1993**, *26*, 615; b) D. Stalke, *Chem. Soc. Rev.* **1998**, *27*, 171.

[24] Bruker APEX v2.1-0, Bruker AXS Inst. Inc., Madison (WI, USA), **2007**.

[25] SAINT v7.23A in Bruker APEX v2.1-0, Bruker AXS Inst. Inc., Madison (WI, USA), **2005**.

[26] G. M. Sheldrick, SADABS 2006/4, Göttingen, **2006**.

[27] G. M. Sheldrick, SHELXS in SHELXTL v6.12, Bruker AXS Inst. Inc., Madison (WI, USA), **2000**.

[28] G. M. Sheldrick, *Acta Crystallogr. Sect. A* **2008**, *64*, 112.

[29] N. K. Hansen, P. Coppens, *Acta Crystallogr. Sect. A* **1978**, *34*, 909.

[30] A. Volkov, P. Macchi, L. J. Farrugia, C. Gatti, P. R. Mallinson, T. Richter, T. Koritsanszky, XD2006, A Computer Program Package for Multipole Refinement, Topological Analysis of Charge Densities and Evaluation of Intermolecular Energies from Experimental or Theoretical Structure Factors, **2006**.

[31] R. Ahlrichs, M. Bär, M. Häser, H. Horn, C. Kölmel, *Chem. Phys. Lett.* **1989**, *162*, 165.

[32] F. Biegler-König, J. Schönbohm, D. Bayles, *J. Comput. Chem.* **2001**, *22*, 545.